Structural, optical and dielectric properties of relaxor-ferroelectric $Pb_{0.78}Ba_{0.22}Sc_{0.5}Ta_{0.5}O_3$

2006 J. Phys.: Condens. Matter 18 L385

(http://iopscience.iop.org/0953-8984/18/31/L01)

INSTITUTE OF PHYSICS PUBLISHING JOURNAL OF PHYSICS: CONDENSED MATTER

J. Phys.: Condens. Matter **18** (2006) L385–L393 doi:10.1088/0953-8984/18/31/L01

LETTER TO THE EDITOR

Structural, optical and dielectric properties of relaxor-ferroelectric $Pb_{0.78}Ba_{0.22}Sc_{0.5}Ta_{0.5}O_3$

V Marinova[1,5], B Mihailova[1,6], T Malcherek[1], C Paulmann[1], K Lengyel[2], L Kovacs[2], M Veleva[3], M Gospodinov[3], B Güttler[4], R Stosch[4] and U Bismayer[1]

[1] Mineralogisch-Petrographisches Institut, Grindelallee 48, Universität Hamburg, D-20146 Hamburg, Germany
[2] Research Institute of Solid State Physics and Optics, Hungarian Academy of Sciences, H-1525 Budapest, PO Box 49, Hungary
[3] Institute of Solid State Physics, Bulgarian Academy of Sciences, Boulevard Tzarigradsko Chausse 72, 1784 Sofia, Bulgaria
[4] Physikalisch-Technische Bundesanstalt, Bundesallee 100, 38116 Braunschweig, Germany

E-mail: mi0a007@uni-hamburg.de

Received 29 May 2006, in final form 24 June 2006
Published 21 July 2006
Online at stacks.iop.org/JPhysCM/18/L385

Abstract

We report on the synthesis of a new relaxor compound with chemical formula $Pb_{0.78}Ba_{0.22}Sc_{0.5}Ta_{0.5}O_3$ (PBST). Single crystals were obtained by the high-temperature solution growth method. The structure of the new compound is of double-perovskite type with face-centred cubic symmetry at room temperature. The frequency dependence of the dielectric constant of PBST shows a strong dielectric dispersion in a wide temperature range and a dielectric-constant maximum near 200 K at 10 kHz. The local atomic environment was probed by Raman scattering and optical absorption spectroscopy. The results show that the incorporation of Ba deforms the BO_6 octahedra adjoining the BaO_{12}-polyhedra along the ⟨111⟩ direction and shortens the Pb–O bond lengths next to the BaO_{12}-polyhedra within the {111} planes. The random substitution of Ba for Pb leads to a wider distribution in the size and shape of the ferroic species in PBST compared to stoichiometric $PbSc_{0.5}Ta_{0.5}O_3$. The addition of Ba shifts the optical absorption edge to lower energies and gives rise to extra absorption peaks at 460 and 730 nm. The latter peak is related to polar atomic rearrangements in the vicinity of the Ba ions embedded into the $PbSc_{0.5}Ta_{0.5}O_3$ matrix.

[5] On leave from: Central Laboratory of Optical Storage and Processing of Information, Bulgaria.
[6] Author to whom any correspondence should be addressed.

1. Introduction

Pb-based perovskites with the general formula $Pb(B'_xB''_{1-x})O_3$ are typical representatives of relaxor ferroelectrics: they possess high dielectric permittivity; a broad, diffuse phase transition over a temperature range; and a strong frequency dependence of the dielectric permittivity as a function of temperature. The excellent dielectric properties, together with the strong electrostriction, which is important for actuators, and the large electro-optic coefficient, which is useful for optical modulators and information storage, open up a wide range of industrial applications [1].

Generally, relaxor-type materials may undergo transitions between (i) a proper paraelectric state; (ii) a paraelectric ergodic state characterized by the occurrence of randomly oriented polar nano-regions; (iii) an intermediate non-ergodic state ('true' relaxor state) characterized by the presence of coupled polar nano-regions but the absence of long-range ferroelectric (FE) order; and (iv) a proper ferroelectric state. The polar nano-regions nucleate at high temperatures beyond the Curie temperature range and at the ergodic state they are characterized by high mobility and random fluctuation between energetically equivalent states [2]. Upon cooling, the dipole dynamics becomes frozen, i.e. the system transfers into the non-ergodic state. Different theoretical approaches have been developed to explain the unusual dielectric properties of relaxors, including superparaelectric- and dipolar-glassy modes, proposing thermal fluctuations of independent and interacting polar clusters, respectively [3, 4], random field-stabilized domain state models, proposing size-restricted nanodomains due to the existence of local electric fields [5], etc. A common feature of the various models is that they are all based on the concept of a large distribution in size and shape of the existing polar regions responsible for the wide, broad peak in the temperature dependence of the dielectric constant.

Among the B-site complex systems of type $Pb(B'_xB''_{1-x})O_3$ compounds with $x = 1/3$, $PbMg_{1/3}Nb_{2/3}O_3$ (PMN) and $PbZn_{1/3}Nb_{2/3}O_3$ are 'classical' relaxors [6]. They exhibit strong frequency dispersion of the dielectric permittivity and no structural anisotropy even at temperatures significantly below the temperature of the dielectric-constant maximum T_m. On cooling, in these systems the incipient polar nanodomains never become large enough to precipitate into a long-range ordered FE state [3]. Thus only the application of an external electric field [7] or hydrostatic pressure [8] can induce a phase transition from a non-ergodic state to a proper FE state. In systems with $x = 1/2$, such as $PbSc_{1/2}Nb_{1/2}O_3$ (PSN) and $PbSc_{1/2}Ta_{1/2}O_3$ (PST), a spontaneous phase transition from a non-ergodic relaxor to a long-range ordered FE state occurs without the application of any external field [9]. The stabilization of the relaxor state in PST and PSN crystals, similar to those observed in PMN, is still a problematic issue and several solutions have been proposed to resolve it. Chu *et al* [10] suggested varying the degree of the B-site-cation ordering by a suitable thermal annealing or during the crystal growth. However, even complete disordering of B^{3+} and B^{5+} ions is not sufficient to suppress the spontaneous FE phase formation. Another possibility is to induce a Pb deficiency in B-site disordered PST and PSN, thus aiming to suppress the spontaneous FE transformation by introducing an abundance of Pb vacancies. However, a proper FE phase again appears at low temperatures [11, 12]. Furthermore, the existence of Pb vacancies causes additional oxygen vacancies, which are difficult to control. Recently, partial substitution of Ba^{2+} for Pb^{2+} in PSN crystals has been proposed, since the control of Ba ion distribution is easier than that of Pb vacancies [13, 14]. The $Pb_{1-x}Ba_xSc_{0.5}Nb_{0.5}O_3$ composition shows different properties depending on the Ba^{2+} concentration: (i) when the Ba content is less than 4 mol% a spontaneous transition from non-ergodic 'true-relaxor' to a proper FE state occurs upon cooling; (ii) when the Ba content increases to 6–7 mol% the system reaches a morphotropic phase boundary and higher doping stabilizes the non-ergodic state with no

long-range FE ordering [15]. Furthermore, PSN doped with 6 mol% of Ba exhibits better-pronounced relaxor behaviour than B-site-disordered or Pb-vacancy-bearing PSN [16].

In this letter we report on a new Pb-based perovskite-type single crystal with a high content of Ba ions in the $PbSc_{1/2}Ta_{1/2}O_3$ matrix. The properties of this newly synthesized compound were analysed by x-ray diffraction, dielectric measurements, Raman scattering, and optical absorption spectroscopy and compared with those of stoichiometric PST.

2. Experimental details

$Pb_{0.78}Ba_{0.22}Sc_{0.5}Ta_{0.5}O_3$ (PBST) single crystals were grown by the high-temperature solution growth method using a flux solution with composition of $PbO{:}PbF_2{:}B_2O_3 = 0.75{:}0.24{:}0.1$. The ratio between the flux and the crystallizing compound was 7:1. The growing process was performed in platinum crucibles in a temperature range 1475–1193 K with a cooling rate of 0.5 °C h^{-1}. The obtained single crystals are dark-red coloured with well-shaped {100} planes and a linear size of the individual crystals varying between 3 and 10 mm.

The chemical composition was determined by electron microprobe analysis with a Cameca Microbeam SX100 electron probe microanalyser. Standards of vanadinite, marium silicate glass, Sc_2O_3, and Ta_2O_5 were used to determine the content of Pb, Ba, Sc, and Ta, respectively.

The room-temperature crystal structure was probed by x-ray diffraction analysis using a Philips X'Pert diffractometer (Cu Kα radiation, a step width of 0.02° in 2θ, and an accumulation time of 4 s per step). Single-crystal diffraction data were collected at beamline F1 at HASYLAB/DESY, using $\lambda = 0.4$ Å radiation and a MarCCD 165 detector. Integration of intensities was performed using x-ray diffraction spectroscopy (XDS) [17] and the structure was refined using Jana2000 software package [18].

The dielectric measurements were performed in the frequency range 10 kHz–1 Mz using a Hewlett Packard 4275 multi-frequency bridge with a relative error of 2% in the temperature range 120–420 K. The applied voltage was 1 V.

Raman spectroscopic measurements were performed at different temperatures in the range 7–540 K using a triple-grating spectrometer Jobin-Yvon Horiba T64000 equipped with an Olympus BH2 microscope. The Raman scattering was excited with the 514.5 nm line of an Ar^+ laser. The laser power on the sample surface was 10 mW, while the diameter of the laser spot on the sample surface was approximately 2.5 μm. Polarized spectra were collected with a spectral resolution of 2 cm^{-1} in four scattering geometries: $Z(XX)\bar{Z}$, $Z(XY)\bar{Z}$, $Z(X'X')\bar{Z}$ and $Z(X'Y')\bar{Z}$ (Porto's notation), where X, Y, Z, X' and Y' are along the crystallographic [100], [010], [001], [110], and [1$\bar{1}$0] directions, respectively. The measured Raman spectra were subsequently temperature-reduced to account for the Bose–Einstein distribution factor.

Ultraviolet/visible/near-infrared (UV/VIS/NIR) transmittance spectra were measured on double-polished plates with a thickness of 0.9 mm using a Jasco 550 UV–VIS spectrophotometer and a Bruker FT-IR (Fourier transform infrared) spectrometer with a near-infrared extension. The optical spectroscopic measurements were carried out with a spectral resolution of 0.1 nm in the temperature range 8–450 K. Plates with a thickness of less than 180 μm were additionally used for the precise determination of the optical absorption edge at room temperature.

3. Results and discussion

The powder x-ray diffraction analysis revealed the perovksite-type structure and the phase purity of the newly synthesized compound (figure 1). The superlattice Bragg reflections observed in the XRD pattern of PBST (inset in figure 1) indicate the occurrence of long-range

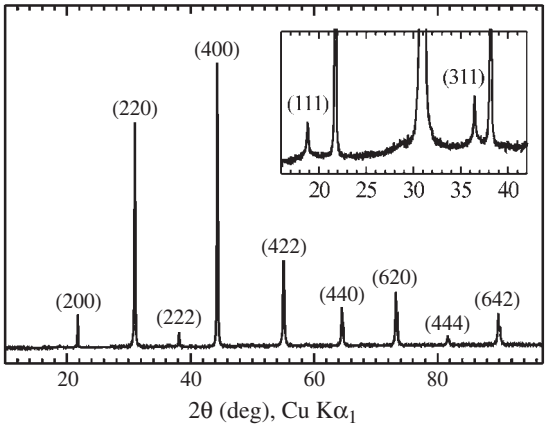

Figure 1. Powder x-ray diffraction pattern of $Pb_{0.78}Ba_{0.22}Sc_{0.5}Ta_{0.5}O_3$ indexed in $Fm\bar{3}m$; the inset displays the superlattice Bragg reflections arising from regions with long-range B-site ordering.

Table 1. Room-temperature fractional atomic coordinates, equivalent isotropic thermal parameters (U_{equiv}) and site occupancy factors (SOF) of $Pb_{0.78}Ba_{0.22}Sc_{0.5}Ta_{0.5}O_3$ refined in $Fm\bar{3}m$, $a = 8.265$ Å; the R-value for 218 observations was 3.87.

Atom	Site	x	y	z	U_{equiv} (Å^2)	SOF
Pb	8c	0.25	0.25	0.25	0.0375(9)	0.82(3)
Ba	8c	0.25	0.25	0.25	0.0375(9)	0.18(3)
Ta	2a	0	0	0	0.0020(2)	0.615(1)
Sc	2a	0	0	0	0.0020(2)	0.385(1)
Ta	2b	0.5	0.5	0.5	0.0020(2)	0.385(1)
Sc	2b	0.5	0.5	0.5	0.0020(2)	0.615(1)
O	24e	0.2482(2)	0	0	0.015(1)	0.95(5)

B-site ordering. The approximate size of the long-range B-site ordered domains determined from the width of the superlattice reflection according to the Scherrer equation is 33 nm. The single-crystal diffraction analysis validates that at room temperature the structure of PBST is face-centred cubic with a unit cell parameter of 8.265 Å (table 1). Within the experimental error the atomic occupation factors are in accordance with the electron-microprobe results. The degree of B-site ordering calculated from the refined site occupancy factors as $\frac{|SOF(Ta)-SOF(Sc)|}{SOF(Ta)+SOF(Sc)}$ is 0.23. One should mention that a satisfactory R-value was obtain after releasing the anharmonic temperature factors at the Pb site up to sixth order.

The temperature dependences of the dielectric relative permittivity ε_r and dielectric losses $\tan\delta$ at different frequencies are shown in figure 2. The broad maximum near 200 K (at $f = 10$ kHz) with a well-pronounced diffuse character as well as the substantial frequency dispersion of the dielectric permittivity indicates unambiguously that the newly synthesized PBST is a relaxor ferroelectric. Furthermore, the frequency increase shifts T_m to higher temperatures and reduces the magnitude of the dielectric constant maximum, which is also typical for relaxor ferroelectrics. The strong dielectric dispersion at temperatures below T_m indicates that the addition of Ba strongly affects the dielectric permittivity behaviour and modifies the phase transition, enlarging the temperature interval of intermediate non-ergodic state. The incorporation of Ba results in A-site compositional disorder and enhances the structural defects responsible for the dipole-dynamics freezing. Obviously, upon cooling, the

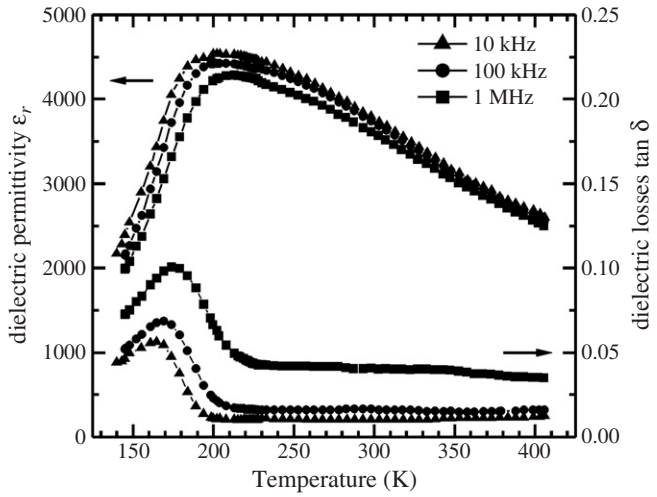

Figure 2. Temperature dependence of the relative permittivity and dielectric losses of $Pb_{0.78}Ba_{0.22}Sc_{0.5}Ta_{0.5}O_3$ measured at 10 kHz, 100 kHz and 1 MHz.

dipoles relax very slowly and PBST shows a typical canonical relaxor behaviour at which polar nano-regions become almost frozen. The dielectric loss variation with temperature exhibits a broad, rounded peak at temperatures below T_m, which shifts to higher temperatures when the probe frequency increases. The occurrence of such a band is typical for canonic relaxors and it is a signature of dipolar relaxation. It is due to the enlargement and orientation of the exciting polar nano-regions and the further nucleation of polar clusters, which increase the density of boundaries between the polar and non-polar regions [19]. The $\tan\delta$-values increase with increasing frequency, which is also characteristic for the relaxors [20]. The observed smooth phase transition and frequency dispersion is similar to Ba-doped PSN crystal, where the increase in the Ba content leads to a decrease in T_m and an increase in the relaxation dynamics during the phase transition [14]. Likewise, Pb-free compounds such as $BaTi_{0.65}Zr_{0.35}O_3$ exhibit a lower T_m and a broader dielectric-constant maximum compared to the Pb-based materials [16]. One can assume that substitution of Ba ions for Pb hinders the dipolar interactions which should overcome the random electric fields and give rise to a long-range ordered FE state and, thus, favours the non-ergodic 'true-relaxor' behaviour in a large temperature range.

The changes in the local structure induced by the incorporation of Ba in the lattice were analysed by Raman spectroscopy. Figure 3 shows the $Z(XX)\bar{Z}$, $Z(XY)\bar{Z}$ spectra of PST and of newly synthesized PBST measured at temperatures well above and below the corresponding temperatures of the dielectric-constant maximum. Generally, the high-temperature phase of PBST exhibits the same spectral peculiarities as those observed for $PbSc_{0.5}B''_{0.5}O_3$ ($B'' = Ta$, Nb) and attributed to the allowed Raman-active modes in $Fm\bar{3}m$ and 'dirty' modes related to the existing nano-sized ferroic clusters [21, 22]. However, there are several distinctions between PBST and PST resulting from the presence of Ba:

(i) A change in the ratio between the two signals in the range 300–370 cm^{-1}, which is related to the correlation length of coherent Pb-shifts along $\langle 111 \rangle$ directions [21, 22]. The smaller intensity ratio between the higher- and the lower-wavenumber components reveals a shorter correlation length for PBST compared to PST.

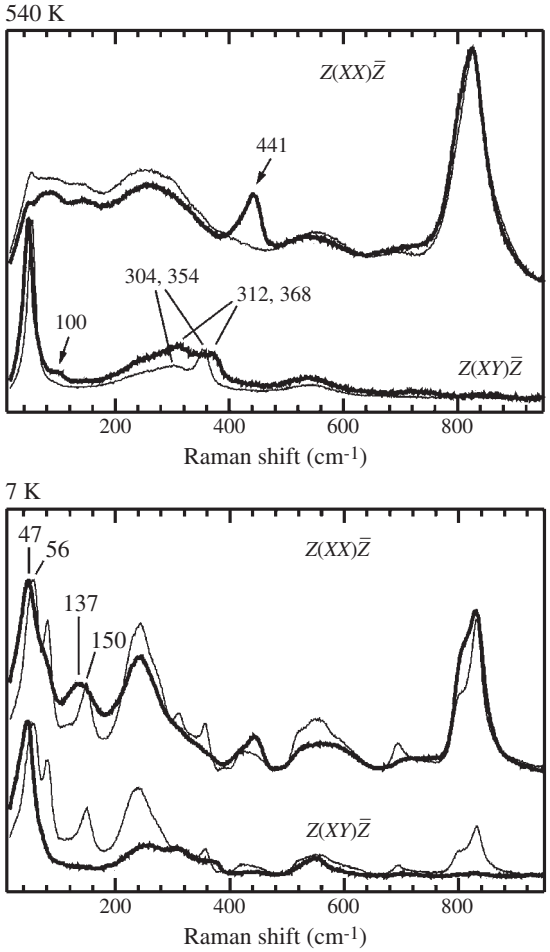

Figure 3. Polarized Raman spectra of $Pb_{0.78}Ba_{0.22}Sc_{0.5}Ta_{0.5}O_3$ (bold lines) and $PbSc_{0.5}Ta_{0.5}O_3$ (thin lines) measured at 540 and 7 K; the spectra are vertically shifted for comparison.

(ii) The appearance of a well-pronounced peak at 441 cm^{-1} in the $Z(XX)\bar{Z}$ spectrum. The Raman scattering in this spectral range is attributed to BO_6-octahedral bending modes [21]. It is observed for the high-temperature phase due to the existence of ferroic clusters inside the paraelectric matrix, i.e. due to local structural fluctuations from the cubic phase. The degree of structural deviations correlates with the intensity of the consequential extra peaks. Hence, intensification of Raman scattering near 440 cm^{-1} indicates additional variation in O–B–O bond angles of the BO_6 octahedra adjoining a Ba and a Pb cation, which is caused by the difference in the PbO_{12}- and BaO_{12}-polyhedral size (see figure 4).

(iii) A shift of the two peaks in the range 300–370 cm^{-1}, which are related to the Pb–O bond stretching modes [21], to higher wavenumbers. This spectral feature is also due the enlarged size of the AO_{12} polyhedron when the A-site is occupied by Ba, thus leading to shortening of the adjacent Pb–O bonds.

(iv) A lower-energy shift of the peak near 55 cm^{-1} originating from the Pb-localized mode. It is observed for both high- and low-temperature phases. This spectral change is most probably due to weakening of the short-range A–O–A bond bending interaction, when Ba

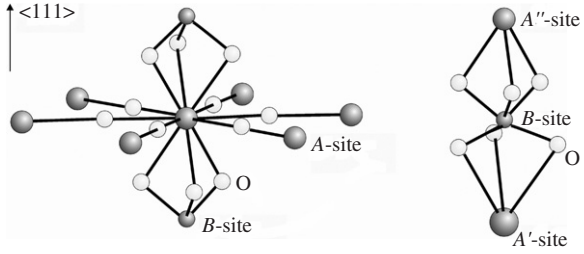

Figure 4. The atomic environment of an A-site cation and of a B-site cation neighbouring two different A-site cations with ionic radii $r_i(\mathrm{A}') > r_i(\mathrm{A}'')$. The effective ionic radii of two-valence 12-coordinated Ba and Pb are 1.61 and 1.49 Å, respectively [23]. The swelling of the AO_{12} polyhedron when Ba substitutes for Pb should result in a shortening of the adjacent Pb–O bonds in the plane perpendicular to ⟨111⟩ direction as well as to a deformation of the adjacent BO_6 octahedra along the ⟨111⟩ direction.

partially substitutes for Pb. The interactions between Ba and O are of more ionic character than those between Pb and O and, therefore, the preferential direction of bonding is less pronounced. Similarly, one should expect weakening of the A–O–B interactions and, as a consequence, lower-energy shift to the corresponding modes, which is indeed observed for the Raman scattering near 150 cm^{-1}, originating from motion of the BO_3 species with respect to the Pb ions [21].

(v) The appearance of an additional peak near 100 cm^{-1} in the $Z(XY)\bar{Z}$ spectrum. The peak is better pronounced in the spectra measured at temperatures higher than $T_\mathrm{m} \sim 200$ K. Thus we suggest that this peak is directly related to the presence of Ba and indicates a two-mode behaviour of the A-cation-localized F_{2g} mode in the paraelectric phase of $Fm\bar{3}m$ symmetry.

Thus the Raman spectroscopic data reveal local structural changes around the Ba cations randomly distributed at the A-sites. These local structural distortions violate the correlation length of coherent Pb shifts with respect to the oxygen layers parallel to the cubic {111} planes and disturb the orientational order of electronic lone-pairs of Pb atoms. The latter is in agreement with the seemingly strong anharmonic temperature movement of the lead atoms obtained from the single-crystal structure refinement. Hence, the incorporation of Ba into the crystal lattice leads to fragmentation of the incipient ferroic species, i.e. to a large distribution over size and shape of the polar clusters occurring within the Curie range. This fact explains the rather broad maximum of temperature dependence of the dielectric permittivity. The Raman spectra of PBST preserve their polarization on cooling, which indicates that a large part of the substance remains in a pseudo-cubic state. Thus the low-temperature phase can be thought of as consisting of small-sized polar clusters of a wide range of structural variation, randomly distributed in an isotropic matrix.

The optical transmittance spectrum of PBST is characterized by a wide transmittance range from 0.36 to 6 μm (figure 5). As can be seen, the addition of Ba significantly shifts the transmittance shoulder to the near-infrared region compared to PST. PBST shows a well-defined broad absorption shoulder extending from the band edge at 3.4 eV and up to 1.1 eV. The shift of the PBST energy gap E_g from 3.2 eV for PST to 3.4 eV for PBST shows that the electron properties and band structures of the two compositions are rather different. The increased structural disorder and the occurrence of A-site compositional disorder reduce the optical gap. The appearance of two additional absorption peaks in the visible spectral range, located at 460 and 730 nm, is evident for different inter-band transitions in PBST compared to

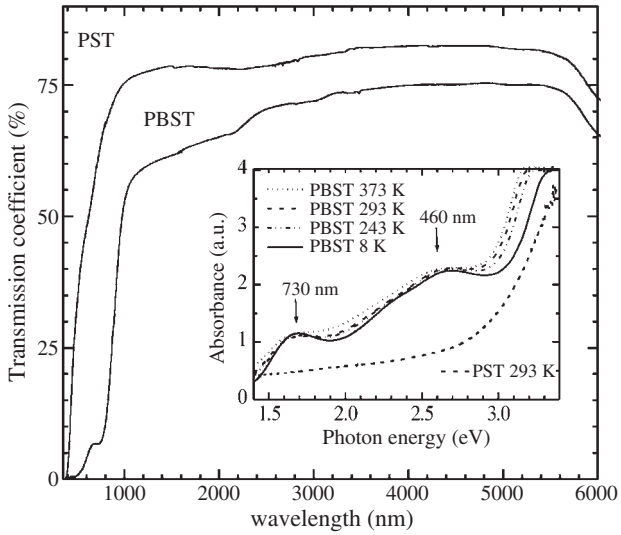

Figure 5. Room-temperature optical transmittance spectra of PBST and PST; the inset shows the corresponding absorbance spectra in the visible range measured at different temperatures.

PST. Most probably, the extra optical peaks are related to the local structural defects created by the Ba atoms. We suppose that the incorporation of Ba ions increases the concentration of effective trap centres and, consequently, the absorption through the investigated spectral range. The increased absorption around 460 nm is most probably due to the existence of deep defect levels. The optical absorption measured at different temperatures is presented in the inset of figure 5. For a temperature decrease, the absorption edge shifts towards higher energies, which is typical for ferroelectric materials [24]. The absorption peak detected at 760 nm shows an anomalous strengthening in the low-temperature range of the non-ergodic state. Generally, optical absorption decreases on cooling due to the suppression of the electron thermal mobility. On the other hand, in relaxors the temperature decrease enhances the development of polar regions. Thus, the temperature behaviour of the peak at 760 nm indicates that it originates from electron-state transitions in ferroic species, the formation of which is provoked by the substitution of Ba for Pb.

4. Conclusion

The newly synthesized single-crystal compound $Pb_{0.78}Ba_{0.22}Sc_{0.5}Ta_{0.5}O_3$ is a relaxor ferroelectric with perovskite-type structure, possessing a cubic symmetry with a $Fm\bar{3}m$ space group at room temperature. The substitution of Ba for Pb causes local structural alterations consisting of deformation of the BO_6 octahedra adjoining the BaO_{12}-polyhedra along the $\langle 111 \rangle$ direction and of shortening of the Pb–O bond lengths next to the BaO_{12}-polyhedra within the {111} planes. The lack of periodicity in the Ba incorporation leads to fragmentation and randomization of the ferroic species typical of stoichiometric $PbSc_{0.5}Ta_{0.5}O_3$. As a result, the non-ergodic 'true-relaxor' state is enhanced on account of the proper long-range ordered ferroelectric state, which considerably broadens the dielectric-constant maximum and modifies the optical absorption edge.

Financial support from the Deutsche Forschungsgemeinschaft (MI 1127/1-1) is gratefully acknowledged. MG, BM and MV are indebted to NSF-BMES (NT 1-02).

References

[1] Cross L E 1994 *Ferroelectrics* **151** 305
[2] Bokov A A and Ye Z G 2006 *J. Mater. Sci.* **41** 31
[3] Smolenskii G A 1970 *J. Phys. Soc. Japan* **28** 26
[4] Viehland D, Jang S J, Cross L E and Wuttig M 1990 *J. Appl. Phys.* **68** 2916
[5] Westphal V, Kleemann W and Glinchuk M D 1992 *Phys. Rev. Lett.* **68** 847
[6] Cross L E 1987 *Ferroelectrics* **76** 241
[7] Arndt H, Sauerbier F, Schmidt G and Shebakov L A 1988 *Ferroelectrics* **79** 145
[8] Samara G A 1996 *Phys. Rev. Lett.* **77** 314
[9] Setter N and Cross L E 1980 *J. Appl. Phys.* **51** 4356
[10] Chu F, Reaney I M and Setter N 1994 *Ferroelectrics* **151** 343
[11] Chu J, Setter N and Tagantsev A K 1993 *J. Appl. Phys.* **74** 5129
[12] Chu F, Reaney I M and Setter N 1995 *J. Appl. Phys.* **77** 1671
[13] Raevski I P, Eremkin V V, Smotrakov V G, Gagarina E S and Maliskaja M A 2000 *Phys. Solid State* **42** 161
[14] Malibert C, Dkhil B, Kiat J M, Durand D, Berar J F and Spasojevic-de Bire A 1997 *J. Phys.: Condens. Matter* **9** 7485
[15] Kamzina L S, Raevski I P, Eremkin V V and Smotrakov V G 2002 *Phys. Solid State* **44** 1754
[16] Sciau Ph, Calvarin G and Ravez J 2000 *Solid State Commun.* **113** 77
[17] Kabsch W 1993 *J. Appl. Crystallogr.* **26** 795
[18] Petricek V, Dusek M and Palatinus L 2000 Jana2000. The crystallographic computing system, Institute of Physics, Praha, Czech Republic
[19] Budault O, Perrin C, Caranoni C and Menguy N 2001 *J. Appl. Phys.* **90** 4115
[20] Shrout T R and Fielding J Jr 1991 *Ultrasonics Symposium Proceedings IEEE 1990* vol 2, p 711
[21] Mihailova B, Bismayer U, Güttler B, Gospodinov M and Konstantinov L 2002 *J. Phys.: Condens. Matter* **14** 1091
[22] Mihailova B, Bismayer U, Güttler B, Gospodinov M, Boris A, Bernhard C and Aroyo M 2005 *Z. Kristallogr.* **220** 740
[23] Liebau F 1985 *Structural Chemistry of Silicates* (Berlin: Springer) p 305
[24] Lines M E and Glass A M 1977 *Principles and Applications of Ferroelectrics and Related Materials* (Oxford: Clarendon) p 438